Chiral charge order in $1T$-$TiSe_2$: importance of lattice degrees of freedom

B. Zenker[1], H. Fehske[1], H. Beck[2], C. Monney[3], and A. R. Bishop[4]
[1] *Institut für Physik, Ernst-Moritz-Arndt-Universität Greifswald, D-17489 Greifswald, Germany*
[2] *Département de Physique and Fribourg Center for Nanomaterials, Université de Fribourg, CH-1700 Fribourg, Switzerland*
[3] *Fritz-Haber-Institut der Max Planck Gesellschaft, Faradayweg 4-6, 14195 Berlin, Germany*
[4] *Theory, Simulation, and Computation Directorate, Los Alamos National Laboratory, Los Alamos, New Mexico 87545, USA*

(Dated: April 9, 2013)

We address the question of the origin of the recently discovered chiral property of the charge-density-wave phase in $1T$-$TiSe_2$ which so far lacks a microscopic understanding. We argue that the lattice degrees of freedom seems to be crucial for this novel phenomenon. We motivate a theoretical model that takes into account one valence and three conduction bands, a strongly screened Coulomb interaction between the electrons, as well as the coupling of the electrons to a transverse optical phonon mode. The Falicov-Kimball model extended in this way possesses a charge-density-wave state at low temperatures, which is accompanied by a periodic lattice distortion. The charge ordering is driven by a lattice deformation and electron-hole pairing (excitonic) instability in combination. We show that in addition an explicit phonon-phonon interaction must be taken into account to achieve a stable chiral charge order. The chiral property is exhibited in the ionic displacements. Exploring the interplay between electron-electron interaction and the electron-phonon coupling in the whole parameter regime, we provide the ground-state phase diagram of the model and give an estimate of the electron-electron and electron-phonon interaction constants for $1T$-$TiSe_2$.

PACS numbers: 71.45.Lr, 71.27.+a, 63.20.kk, 71.35.Lk, 71.38.-k

I. MOTIVATION

Charge-density-waves (CDWs) brought about by electron-phonon[1] or electron-electron[2] interactions are broken-symmetry ground states, typically of low-dimensional (D) solids with anisotropic properties.[3] A prominent material exhibiting such a periodic real-space modulation of its charge density is the transition-metal dichalcogenide $1T$-$TiSe_2$. This quasi-2D system undergoes a structural phase transition at about 200 K, at which a commensurate $2 \times 2 \times 2$ superstructure accompanied by a CDW develops.[4] Thereby the CDW features three coexisting components and, for this reason, is denoted as triple CDW. Although the charge ordered phase in $1T$-$TiSe_2$ has been a matter of intensive research for more than three decades, the driving force behind the phase transition has not been identified conclusively.

Recent experiments on $1T$-$TiSe_2$, pointing to a very unusual chiral property of the CDW, have reinforced the interest in this problem.[5,6] An object exhibits chirality if it cannot be mapped on its mirror image solely by rotations and translations. For a CDW phase characterized by a scalar quantity such chirality has not been detected before. The scanning tunneling microscopy measurements performed by Ishioka and co-workers, however, show that the amplitude of the tunneling current modulates differently along the CDW unit vectors in $1T$-$TiSe_2$.[5] Since the tunneling-current amplitude directly measures the local electron density, the charge density modulates differently along the three unit vectors. As a result the material in its low-temperature phase will not exhibit a three-fold symmetry as suggested by the triangular lattice structure. The Fourier transformation of the scanning tunneling microscopy data demonstrates a triple CDW as well as a different charge modulation along each CDW component with the respective ordering vector Q_α, $\alpha = 1, 2, 3$.[5] If one orders the triple-CDW components according to their charge modulation amplitude in ascending order, in a sense a direction is induced and the triple CDW exhibits chirality because the mirror symmetry is broken, in contrast to usual CDWs;[6] see the schematic representation by Fig. 1. Note that clockwise and anticlockwise chiral CDWs were found in the same sample, suggesting that these states are degenerate. This

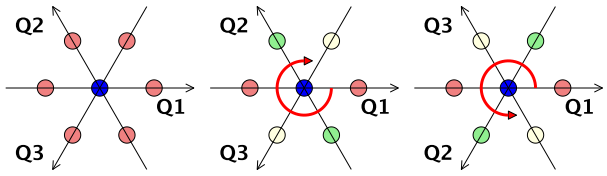

(a) nonchiral (b) clockwise (c) anticlockwise

FIG. 1. (color online) Electron-density pattern for a triangular lattice in case of (a) a nonchiral CDW or (b,c) chiral CDWs. Filled circles picture the value of the charge densities, where equal colors mark equal densities. For the nonchiral CDW shown in (a) the density modulation along the ordering vectors $\mathbf{Q}_1$, $\mathbf{Q}_2$, and $\mathbf{Q}_3$ is equal. Reflection along an ordering vector yields the same density pattern, i.e., mirror symmetry exists. The situation changes for a chiral CDW. A clockwise CDW (red arrow) is illustrated in (b). Now reflexion along $\mathbf{Q}_1$ yields the situation depicted in panel (c). Obviously the pattern (c) describes an anticlockwise CDW: That is, for a chiral CDW mirror symmetry is broken.

two-fold symmetry is corroborated by optical polarimetry measurements.[5] Ishioka and co-workers furthermore noticed that the experimental data can be reproduced by a charge density modulation of the form

$$n_i(\mathbf{Q}_\alpha) = A\cos(\mathbf{Q}_\alpha \mathbf{R}_i + \theta_\alpha), \tag{1}$$

where A is the modulation amplitude and θ_α are initial phases.[5] For a chiral CDW to exist the phases of the CDW components must differ, i.e., $\theta_1 \neq \theta_2 \neq \theta_3$.

From a theoretical point of view the chiral CDW in 1T-$TiSe_2$ was addressed by a Landau-Ginzburg approach.[7,8] Thereby the relative phases of the CDW order parameters were obtained by minimizing the free energy functional. Two CDW transitions were found with decreasing temperature: Firstly a standard (nonchiral) CDW appears, and subsequently a chiral CDW emerges, i.e., $T_{\text{nonchiral CDW}} > T_{\text{chiral CDW}}$. Within the CDW phase three distinct orbital sectors are occupied, leading to an orbital-ordered state and three interacting lattice displacement waves (with different polarizations).

An open issue is the microscopic mechanism driving the CDW transition. Basically two scenarios were discussed in the literature, where the charge order results from purely electronic, respectively electron-lattice, correlations. Angle-resolved photoemission spectroscopy data reveal a relatively large transfer of spectral weight from the original bands to the back-folded bands (due to the CDW transition), compared with the small ionic displacement. This suggests an electronic mechanism within the excitonic insulator (EI) scenario.[9,10] A corresponding tight-binding calculation estimates the amplitude of the lattice deformation caused by an EI instability to be of the same order as the measured one.[11] The gradual suppression of the CDW phase by changing solely electronic properties by intercalation with S or Te further corroborates the EI concept.[12] Most convincingly, time-resolved photoemission spectroscopy reveals an extremely fast response of the CDW to external light pulses which favors an electronic mechanism.[13] Alternatively, the coupling to the lattice degrees of freedom may drive the CDW transition, e.g., by a cooperative Jahn-Teller effect.[14,15] Here the particular form of the phonon dispersion and the softening of transverse optical phonon modes were elaborated within a tight-binding approach and found to agree with the experimental results.[16–19] The same holds for an ab-initio approach[20] to a Jahn-Teller effect. Likewise the onset of superconductivity by applying pressure may be understood within a phonon-driven CDW scenario.[21] Since some properties of the CDW in 1T-$TiSe_2$ can be understood by the excitonic condensation of electron-hole pairs and others by the instability of a phonon mode, a combined scenario has been proposed.[22]

As yet it is unclear whether the chiral property of the CDW favors the electronic or lattice scenario, or a combination of both. In the present work, this issue is addressed amongst others. We start by investigating the CDW from an EI perspective. The corresponding mean-field approach for an extended Falicov-Kimball model is presented in Sec. II A. We show that the EI scenario is insufficient to explain a stable chiral CDW. We proceed by including the lattice degrees of freedom. It turns out that, besides an electron-phonon coupling, the phonon-phonon interaction has to be taken into account in order to stabilize chiral charge order. This is elaborated in Sec. II B. The self-consistency equations for the CDW and EI order parameters are derived in Sec. II C. The CDW state is characterized analytically in Sec. II D. Section III contains our main (numerical) results. Here we give the functional dependences of the EI order parameter and the lattice distortion on the model parameters and temperature, derive the ground-state phase diagram, and estimate the interaction constants for 1T-$TiSe_2$. In Sec. IV, we summarize and conclude.

II. MODEL AND THEORETICAL APPROACH

A. Electronic degrees of freedom

1. *Band structure*

Since the electronic properties of 1T-$TiSe_2$ are dominated by the electrons near the Fermi energy, in what follows we only take into account the top valence band and the lower conduction band. The maximum of the valence band is located at the Γ-point. The conduction band exhibits minima at the three L-points, see Fig. 2. To facilitate the notation, we artificially split the conduction band into three symmetry-equivalent bands indexed by α, each having one minimum at the point L_α. The band dispersions of these three conduction bands mimics the true band structure close to the L-points.[10] Figure 3 illustrates the situation close to the Fermi level. Then the free electron part is written as

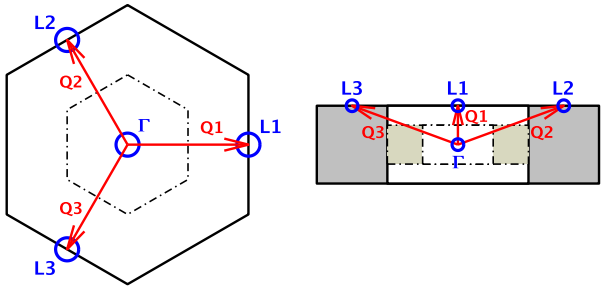

FIG. 2. (color online) First Brillouin zone (BZ) of 1T-$TiSe_2$ with high symmetry points in the normal phase (solid line) and in the CDW phase (dot-dashed line). Red arrows show the CDW ordering vectors. Left panel: projection onto the xy-plane, right panel: projection onto the yz-plane.

$$H_{\text{e}} = \sum_{\mathbf{k}} \varepsilon_{\mathbf{k}f} f^\dagger_{\mathbf{k}} f_{\mathbf{k}} + \sum_{\mathbf{k},\alpha} \varepsilon_{\mathbf{k}\alpha} c^\dagger_{\mathbf{k}\alpha} c_{\mathbf{k}\alpha}, \tag{2}$$

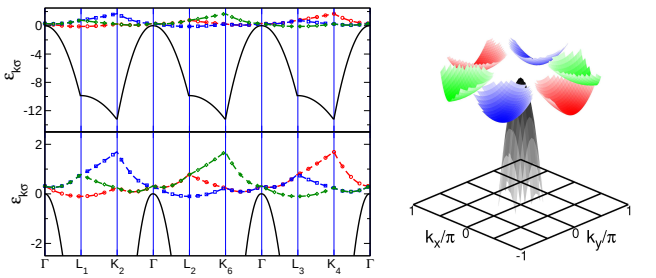

(a)band structure along high-symmetry directions of the BZ

(b)band dispersion close to the Fermi level

FIG. 3. (color online) Model band structure in the normal phase. The valence band is colored in black and the conduction bands are colored red, blue, and green.

where $f_{\mathbf{k}}^{(\dagger)}$ annihilates (creates) an electron in the valence band with momentum $\mathbf{k}$ and $c_{\mathbf{k}\alpha}^{(\dagger)}$ annihilates (creates) an electron in the conduction band with momentum $\mathbf{k}$ and band index α. The corresponding valence-band dispersion and the conduction-band dispersions are denoted as $\varepsilon_{\mathbf{k}f}$ and $\varepsilon_{\mathbf{k}\alpha}$. They will be specified in Sec. III A. The spin of the electrons is neglected.

Taking the band structure and a band filling factor $n = 1/4$ into account, $1T$-$TiSe_2$ resides in the vicinity of a semimetal-semiconductor transition, cf. Fig 3. Accordingly the chemical potential μ is determined by

$$n_f + \sum_\alpha n_\alpha = 1, \tag{3}$$

where

$$n_f = \frac{1}{N}\sum_{\mathbf{k}} \langle n_{\mathbf{k}}^f \rangle = \frac{1}{N}\sum_{\mathbf{k}} \langle f_{\mathbf{k}}^\dagger f_{\mathbf{k}} \rangle, \tag{4}$$

$$n_\alpha = \frac{1}{N}\sum_{\mathbf{k}} \langle n_{\mathbf{k}}^\alpha \rangle = \frac{1}{N}\sum_{\mathbf{k}} \langle c_{\mathbf{k}\alpha}^\dagger c_{\mathbf{k}\alpha} \rangle \,. \tag{5}$$

Here N denotes the total number of lattice sites.

Regarding the isotropy (anisotropy) of the valence (conduction) band(s) the Fermi surface of $1T$-$TiSe_2$ is only poorly nested,[15] which rules out a nesting mechanism for the CDW formation even in a simplified 2D setting.

2. *Electron-electron interaction*

Due to the strong screening of the Coulomb interaction in $1T$-$TiSe_2$,[23] we assume a local electron-electron interaction,

$$H_{\mathrm{e-e}} = \frac{U_{cc}}{N}\sum_{\mathbf{k},\mathbf{k}',\mathbf{q}}\sum_{\alpha}\sum_{\beta>\alpha} c_{\mathbf{k}+\mathbf{q}\alpha}^\dagger c_{\mathbf{k}\alpha} c_{\mathbf{k}'\beta}^\dagger c_{\mathbf{k}'+\mathbf{q}\beta} + \frac{U_{fc}}{N}\sum_{\mathbf{k},\mathbf{k}',\mathbf{q}}\sum_{\alpha} f_{\mathbf{k}+\mathbf{q}}^\dagger f_{\mathbf{k}} c_{\mathbf{k}'\alpha}^\dagger c_{\mathbf{k}'+\mathbf{q}\alpha}\,, \tag{6}$$

where U_{cc} denotes the Coulomb repulsion among the conduction electrons. The on-site Coulomb interaction U_{fc} between valence and conduction band electrons determines the distribution of electrons between these "subsystems" and therefore may drive a valence transition, as observed, e.g., in heavy fermion and intermediate-valence Tm[Se,Te] compounds.[24,25] If the total electronic model contains an explicit hybridization between f and c electrons[26,27] or, as in our case, dispersive c *and* f bands,[28] coherence between c and f particles can develop. Then U_{fc} may lead to a pairing of c-band electrons and f-band holes, i.e., to the formation of excitons and, provided a large enough number of excitons is created, a subsequent spontaneous condensation of these composite quasiparticles may develop. In real systems this excitonic instability is expected to occur, when semimetals with very small band overlap or semiconductors with very small band gap are cooled to extremely low temperatures.[29,30] The excitonic condensate then typifies a macroscopic phase-coherent insulating state, the EI, which separates the semimetal from the insulator.[31,32] From a theoretical point of view, Falicov-Kimball-type models seem to be the most promising candidates for realizing collective exciton phases. This holds particularly for the generic two-band extended Falicov-Kimball model (EFKM), where an EI ground state has been proven to exist in 1D and 2D by constrained-path Monte Carlo simulations.[28,33] Subsequent Hartree-Fock, slave-boson and projector-based renormalization techniques yield the 2D EFKM ground-state phase diagram in even quantitative accordance with unbiased Monte Carlo data,[34–42] supporting the applicability of these analytical approaches also in 3D and for more complicated situations.

The electronic part of our Hamiltonian,

$$H_{\mathrm{mEFKM}} = H_{\mathrm{e}} + H_{\mathrm{e-e}}, \tag{7}$$

can be viewed as a multiband extended Falicov-Kimball model (mEFKM). We note that the mEFKM was studied previously and has been shown to reproduce the angle-resolved photoemission spectroscopy data for $1T$-$TiSe_2$ at temperatures below the critical temperature[9,10,43–45], as well as above but close to the critical temperature.[23,46]

We note that the mEFKM exhibits a particular U(1) symmetry. This can be seen by applying the unitary transformation $U_{\varphi,\alpha} = e^{i\varphi S_\alpha}$ with $S_\alpha = \frac{1}{2}\sum_i (f_i^\dagger f_i - c_{i\alpha}^\dagger c_{i\alpha})$. The operators $f_i^{(\dagger)}$ and $c_{i\alpha}^{(\dagger)}$ annihilate (create) an electron at Wannier site i. Obviously we have

$$H_{\mathrm{mEFKM}} = U_{\varphi,\alpha}\, H_{\mathrm{mEFKM}}\, U_{\varphi,\alpha}^\dagger \,. \tag{8}$$

This symmetry leads to a degeneracy between chiral and nonchiral CDWs (see below).

To proceed, we perform a Hartree-Fock decoupling of

the electron-electron interaction terms:

$$\frac{U_{cc}}{N}\sum_{\mathbf{k},\mathbf{k}',\mathbf{q}}\sum_{\alpha}\sum_{\beta>\alpha} c^\dagger_{\mathbf{k}+\mathbf{q}\alpha}c_{\mathbf{k}\alpha}c^\dagger_{\mathbf{k}'\beta}c_{\mathbf{k}'+\mathbf{q}\beta} \rightarrow U_{cc}\sum_{\mathbf{k}}\sum_{\alpha}\sum_{\beta\neq\alpha} c^\dagger_{\mathbf{k}\alpha}c_{\mathbf{k}\alpha}n_\beta - NU_{cc}\sum_{\alpha}\sum_{\beta>\alpha} n_\alpha n_\beta\,, \tag{9}$$

$$\begin{aligned}\frac{U_{fc}}{N}\sum_{\mathbf{k},\mathbf{k}',\mathbf{q}}\sum_{\alpha} f^\dagger_{\mathbf{k}+\mathbf{q}}f_{\mathbf{k}}c^\dagger_{\mathbf{k}'\alpha}c_{\mathbf{k}'+\mathbf{q}\alpha} \rightarrow\ & U_{fc}\sum_{\alpha}n_\alpha\sum_{\mathbf{k}}f^\dagger_{\mathbf{k}}f_{\mathbf{k}} + U_{fc}n_f\sum_{\mathbf{k},\alpha}c^\dagger_{\mathbf{k}\alpha}c_{\mathbf{k}\alpha}\\ & - NU_{fc}n_f\sum_{\alpha}n_\alpha - \sum_{\alpha}\Delta_{\mathbf{Q}\alpha}\sum_{\mathbf{k}}c^\dagger_{\mathbf{k}+\mathbf{Q}_\alpha\alpha}f_{\mathbf{k}}\\ & - \sum_{\alpha}\Delta^*_{\mathbf{Q}\alpha}\sum_{\mathbf{k}}f^\dagger_{\mathbf{k}}c_{\mathbf{k}+\mathbf{Q}_\alpha\alpha} + \frac{N}{U_{fc}}|\Delta_{\mathbf{Q}\alpha}|^2\,.\end{aligned} \tag{10}$$

Here we introduced the EI order parameter functions

$$\Delta_{\mathbf{Q}\alpha} = \frac{U_{fc}}{N}\sum_{\mathbf{k}}\langle f^\dagger_{\mathbf{k}}c_{\mathbf{k}+\mathbf{Q}_\alpha\alpha}\rangle, \tag{11}$$

$$\Delta^*_{\mathbf{Q}\alpha} = \frac{U_{fc}}{N}\sum_{\mathbf{k}}\langle c^\dagger_{\mathbf{k}+\mathbf{Q}_\alpha\alpha}f_{\mathbf{k}}\rangle. \tag{12}$$

Since the experiments on $1T$-$TiSe_2$ suggest that the spontaneous hybridization of the valence band with one of the three conduction bands is the dominant effect of the electron-electron interaction,[9] in deriving Eq. (10), we neglected all terms that mix different conduction bands.

The resulting decoupled Hamiltonian takes the form

$$\begin{aligned}\bar{H}_{\mathrm{mEFKM}} =\ & \sum_{\mathbf{k}}\bar{\varepsilon}_{\mathbf{k}f}f^\dagger_{\mathbf{k}}f_{\mathbf{k}} + \sum_{\mathbf{k},\alpha}\bar{\varepsilon}_{\mathbf{k}\alpha}c^\dagger_{\mathbf{k}\alpha}c_{\mathbf{k}\alpha}\\ & - \sum_{\mathbf{k},\alpha}\Delta_{\mathbf{Q}\alpha}c^\dagger_{\mathbf{k}+\mathbf{Q}_\alpha\alpha}f_{\mathbf{k}} - \sum_{\mathbf{k},\alpha}\Delta^*_{\mathbf{Q}\alpha}f^\dagger_{\mathbf{k}}c_{\mathbf{k}+\mathbf{Q}_\alpha\alpha}\\ & - NU_{fc}n_f\sum_{\alpha}n_\alpha - NU_{cc}\sum_{\alpha}\sum_{\beta>\alpha}n_\alpha n_\beta\\ & + \frac{N}{U_{fc}}\sum_{\alpha}|\Delta_{\mathbf{Q}\alpha}|^2\,,\end{aligned} \tag{13}$$

with shifted f and c band dispersions:

$$\bar{\varepsilon}_{\mathbf{k}f} = \varepsilon_{\mathbf{k}f} + U_{fc}\sum_{\alpha}n_\alpha, \tag{14}$$

$$\bar{\varepsilon}_{\mathbf{k}\alpha} = \varepsilon_{\mathbf{k}\alpha} + U_{fc}n_f + U_{cc}\sum_{\beta\neq\alpha}n_\beta\,. \tag{15}$$

The EI low-temperature phase is characterized by non-vanishing expectation values $\langle f^\dagger_{\mathbf{k}}c_{\mathbf{k}+\mathbf{Q}_\alpha\alpha}\rangle$, $\langle c^\dagger_{\mathbf{k}+\mathbf{Q}_\alpha\alpha}f_{\mathbf{k}}\rangle$, which cause a correlation gap in the excitation spectrum. The mean local electron density in the EI phase is

$$n_i = 1 + \frac{2}{N}\sum_{\mathbf{k},\alpha}|\langle c^\dagger_{\mathbf{k}+\mathbf{Q}_\alpha\alpha}f_{\mathbf{k}}\rangle|\cos(\mathbf{Q}_\alpha\mathbf{R}_i + \theta_\alpha), \tag{16}$$

where

$$\frac{1}{N}\sum_{\mathbf{k}}\langle c^\dagger_{\mathbf{k}+\mathbf{Q}_\alpha\alpha}f_{\mathbf{k}}\rangle = \frac{1}{N}\sum_{\mathbf{k}}|\langle c^\dagger_{\mathbf{k}+\mathbf{Q}_\alpha\alpha}f_{\mathbf{k}}\rangle|e^{i\theta_\alpha} = \frac{\Delta^*_{\mathbf{Q}\alpha}}{U_{fc}}. \tag{17}$$

Comparing Eq. (16) with relation (1) we recognize the amplitude of the charge density modulation as the modulus of the hybridization function $\sum_{\mathbf{k}}\langle c^\dagger_{k+Q_\alpha\alpha}f_k\rangle$. Likewise we can identify the initial phases θ_α in the density modulation as the phases of the hybridization functions (which coincide with the phases of the EI order parameters).

Note that previous theoretical studies of the mEFKM[10,11] did not include the phase differences of the θ_α, which will be essential for the establishment of a chiral CDW.[5–8] If one is not concerned with the chiral CDW problem, disregarding the phases θ_α seems to be justified since the U(1) symmetry of the mEFKM prevents the appearance of a stable chiral CDW anyway. We show this by analyzing the behavior of the electron operators under the unitary transformation $U_{\varphi,\alpha}$: $\tilde{c}^{(\dagger)}_{i\alpha} = U_{\varphi,\alpha}c^{(\dagger)}_{i\alpha}U^\dagger_{\varphi,\alpha}$ and $\tilde{f}^{(\dagger)}_i = U_{\varphi,\alpha}f^{(\dagger)}_iU^\dagger_{\varphi,\alpha}$. The hybridization functions (in real space) then transform as $\langle c^\dagger_{i\alpha}f_i\rangle e^{i\mathbf{Q}_\alpha\mathbf{R}_i} = e^{-i\varphi}\langle\tilde{c}^\dagger_{i\alpha}\tilde{f}_i\rangle e^{i\mathbf{Q}_\alpha\mathbf{R}_i}$. That is, the phases θ_α can be controlled by the unitary transformation through the angles φ. However, in view of (8) the total energy is independent of the θ_α. Hence these phases can be chosen arbitrarily and there is no mechanism that stabilizes a given phase difference. Therefore the mEFKM is insufficient to describe a chiral CDW in $1T$-$TiSe_2$. In the following we will demonstrate that the coupling of the electrons to the lattice degrees of freedom can break the U(1)-symmetry of the mEFKM and consequently can stabilize a chiral CDW.

B. Lattice degrees of freedom

1. Electron-phonon coupling

For $1T$-$TiSe_2$ there are experimental and theoretical evidences that the weak periodic lattice distortion observed comes from a softening of a transverse optical phonon mode.[16–20] Of particular importance in this respect is the BZ boundary phonon that connects the Γ- and L_α-points. The valence-band states at the Γ-point and the conduction-band states at the L_α-points are closest to the Fermi energy and, for momentum conservation reasons, the transfer (excitation) of an electron from Γ to L_α should be accompanied by the creation of a phonon with momentum $-\mathbf{Q}_\alpha$. Hence we assume a simplified single-mode electron-phonon interaction that contains only f-c_α band-mixing terms (cf. Ref. 11):

$$\begin{aligned}H_{\mathrm{e-ph}} = \frac{1}{\sqrt{N}}\sum_{\mathbf{k},\mathbf{q}}\sum_{\alpha}\Big[& g^{f\alpha}_{\mathbf{q}}(b^\dagger_{\mathbf{q}} + b_{-\mathbf{q}})f^\dagger_{\mathbf{k}}c_{\mathbf{k}+\mathbf{q}\alpha}\\ & + (g^{f\alpha}_{\mathbf{q}})^*(b^\dagger_{-\mathbf{q}} + b_{\mathbf{q}})c^\dagger_{\mathbf{k}+\mathbf{q}\alpha}f_{\mathbf{k}}\Big]\,.\end{aligned} \tag{18}$$

Here the operator $b_{\mathbf{q}}^{(\dagger)}$ describes the annihilation (creation) of a phonon carrying momentum $\mathbf{q}$, and $g_{\mathbf{q}}^{f\alpha}$ denotes the electron-phonon coupling constant. The Hamiltonian (18) can be derived microscopically following the approach in Ref. 47. Most notably the electron-phonon coupling (18) breaks the U(1) symmetry of the mEFKM, i.e., the arbitrariness with respect to the phases θ_α is eliminated.

2. Phonon-phonon interaction

Within the harmonic approximation, the Hamiltonian for the (noninteracting) phonons reads[48]

$$H_{\rm ph} = \sum_{\mathbf{q}} \hbar\omega(\mathbf{q}) b_{\mathbf{q}}^\dagger b_{\mathbf{q}}\,, \tag{19}$$

where $\omega(\mathbf{q})$ is the bare phonon frequency. A coupling between the lattice vibrations results from the anharmonic contributions in the expansion of the potential for the ions.[49] As we will see below, such an explicit phonon-phonon interaction will be necessary to stabilize the chiral CDW phase. Here we will take into account only terms of cubic and quartic order in the lattice displacement. Then we obtain

$$\begin{aligned} H_{\rm ph-ph} = {}& \frac{1}{\sqrt{N}} \sum_{\mathbf{q}_1,\mathbf{q}_2,\mathbf{q}_3} B(\mathbf{q}_1,\mathbf{q}_2,\mathbf{q}_3)(b_{\mathbf{q}_1}^\dagger + b_{-\mathbf{q}_1}) \\ & \times (b_{\mathbf{q}_2}^\dagger + b_{-\mathbf{q}_2})(b_{\mathbf{q}_3}^\dagger + b_{-\mathbf{q}_3}) \\ & + \frac{1}{N} \sum_{\mathbf{q}_1,\mathbf{q}_2,\mathbf{q}_3,\mathbf{q}_4} D(\mathbf{q}_1,\mathbf{q}_2,\mathbf{q}_3,\mathbf{q}_4)(b_{\mathbf{q}_1}^\dagger + b_{-\mathbf{q}_1}) \\ & \times (b_{\mathbf{q}_2}^\dagger + b_{-\mathbf{q}_2})(b_{\mathbf{q}_3}^\dagger + b_{-\mathbf{q}_3})(b_{\mathbf{q}_4}^\dagger + b_{-\mathbf{q}_4})\,. \end{aligned} \tag{20}$$

The explicit expressions of $B(\mathbf{q}_1,\mathbf{q}_2,\mathbf{q}_3)$ and $D(\mathbf{q}_1,\mathbf{q}_2,\mathbf{q}_3,\mathbf{q}_4)$ are lengthy. We only note the symmetry relations

$$B(-\mathbf{q}_1,-\mathbf{q}_2,-\mathbf{q}_3) = B^*(\mathbf{q}_1,\mathbf{q}_2,\mathbf{q}_3)\,, \tag{21}$$

$$D(-\mathbf{q}_1,-\mathbf{q}_2,-\mathbf{q}_3,-\mathbf{q}_4) = D^*(\mathbf{q}_1,\mathbf{q}_2,\mathbf{q}_3,\mathbf{q}_4)\,, \tag{22}$$

and point out the constraints

$$B(\mathbf{q}_1,\mathbf{q}_2,\mathbf{q}_3) \propto \delta_{\mathbf{q}_1+\mathbf{q}_2+\mathbf{q}_3,\mathbf{G}}\,, \tag{23}$$

$$D(\mathbf{q}_1,\mathbf{q}_2,\mathbf{q}_3,\mathbf{q}_4) \propto \delta_{\mathbf{q}_1+\mathbf{q}_2+\mathbf{q}_3+\mathbf{q}_4,\mathbf{G}}\,. \tag{24}$$

Here $\mathbf{G}$ is a reciprocal lattice vector of the undistorted lattice.

3. Frozen-phonon approach

We now apply the frozen-phonon approximation and calculate the lattice distortion at low temperatures. As elaborated in Refs. 17–20 the phonons causing the lattice displacements in $1T$-$TiSe_2$ have the momenta $\mathbf{Q}_\alpha$ shown in Fig. 2. Their softening is inherently connected to strong electronic correlations.[23] It has been suggested that the $\mathbf{Q}_1$, $\mathbf{Q}_2$, and $\mathbf{Q}_3$ phonons become soft at the same temperature;[18] we therefore assume $|g_{\mathbf{Q}_1}^{f1}| = |g_{\mathbf{Q}_2}^{f2}| = |g_{\mathbf{Q}_3}^{f3}| = g_{\mathbf{Q}}$ (using the notation $g_{\mathbf{Q}_\alpha}^{f\alpha} = g_{\mathbf{Q}} e^{i\Phi_\alpha}$) and $\omega(\mathbf{Q}_1) = \omega(\mathbf{Q}_2) = \omega(\mathbf{Q}_3) = \omega$. A finite displacement of the ions is characterized by $\langle b_{\mathbf{Q}_\alpha}^\dagger\rangle = \langle b_{-\mathbf{Q}_\alpha}\rangle \neq 0$. We denote the static lattice distortions by

$$\delta_{\mathbf{Q}\alpha} = \frac{2}{\sqrt{N}} g_{\mathbf{Q}} \langle b_{\mathbf{Q}_\alpha}\rangle e^{-i\Phi_\alpha} = |\delta_{\mathbf{Q}\alpha}| e^{-i\phi_\alpha}, \tag{25}$$

$$\delta_{\mathbf{Q}\alpha}^* = \frac{2}{\sqrt{N}} g_{\mathbf{Q}} \langle b_{\mathbf{Q}_\alpha}^\dagger\rangle e^{i\Phi_\alpha} = |\delta_{\mathbf{Q}\alpha}| e^{i\phi_\alpha}. \tag{26}$$

Obviously, their phases are composed of two contributions, $\phi_\alpha = \Phi_\alpha + \phi_{b\alpha}$, where Φ_α stems from the phase of the corresponding electron-phonon coupling constant and $\phi_{b\alpha}$ originates from the complex average value $\langle b_{\mathbf{Q}_\alpha}\rangle$. It will become apparent below that $\phi_{b\alpha}$ reflects the interaction between the different CDW components.

If we only take into account the $\mathbf{Q}_\alpha$-phonon modes the cubic terms in $H_{\rm ph-ph}$ vanish, since the finite z-component of the ordering vectors prevents constraint (23) from being satisfied. Hence the first anharmonic corrections are of quartic order. Here the geometry in the xy-plane is crucial. Replacing all phonon operators by their averages, the Hamiltonian $H = H_{\rm e} + H_{\rm e-e} + H_{\rm e-ph} + H_{\rm ph} + H_{\rm ph-ph}$ becomes an effective electronic model:

$$\begin{aligned} \bar{H} = {}& \bar{H}_{\rm mEFKM} + \sum_{\mathbf{k},\alpha} \left(\delta_{\mathbf{Q}\alpha} c_{\mathbf{k}+\mathbf{Q}_\alpha\alpha}^\dagger f_{\mathbf{k}} + \delta_{\mathbf{Q}\alpha}^* f_{\mathbf{k}}^\dagger c_{\mathbf{k}+\mathbf{Q}_\alpha\alpha} \right) \\ & + \frac{DN}{g_{\mathbf{Q}}^4} \sum_\alpha \sum_{\beta>\alpha} \Big[(\delta_{\mathbf{Q}\alpha}^* \delta_{\mathbf{Q}\beta}^*)^2 e^{-2i(\Phi_\alpha+\Phi_\beta)} \\ & + (\delta_{\mathbf{Q}\alpha}\delta_{\mathbf{Q}\beta})^2 e^{2i(\Phi_\alpha+\Phi_\beta)} + (\delta_{\mathbf{Q}\alpha}^*\delta_{\mathbf{Q}\beta})^2 e^{-2i(\Phi_\alpha-\Phi_\beta)} \\ & + (\delta_{\mathbf{Q}\alpha}\delta_{\mathbf{Q}\beta}^*)^2 e^{2i(\Phi_\alpha-\Phi_\beta)} \Big] + \frac{\widetilde{D}}{g_{\mathbf{Q}}^4} \sum_\alpha |\delta_{\mathbf{Q}\alpha}|^4 \\ & + N \sum_\alpha \hbar\omega \frac{|\delta_{\mathbf{Q}\alpha}|^2}{4(g_{\mathbf{Q}})^2}\,. \end{aligned} \tag{27}$$

Here $D = D(\mathbf{Q}_\alpha,\mathbf{Q}_\alpha,\mathbf{Q}_\beta,\mathbf{Q}_\beta)$ $(\beta \neq \alpha)$, $\widetilde{D} = D(\mathbf{Q}_\alpha,\mathbf{Q}_\alpha,-\mathbf{Q}_\alpha,-\mathbf{Q}_\alpha)$, and we assume for simplicity that the phonon-phonon interaction constants are the same for all combinations of α and β. D and $\widetilde{D}$ are real. In Eq. (27), the term proportional to $\tilde{D}$, coming from the expansion of the phonon-phonon interaction, guarantees that the free energy is bounded from below within our approximations. Note that the leading terms of the phonon-phonon interaction expansion relate the phases ϕ_α to each other. Obviously a finite lattice distortion causes a hybridization between the valence and the conduction bands. As a consequence a gap in the electronic spectrum opens, just as in the course of exciton condensation (cf. Eq. (13)). The corresponding local electron density is given by Eq. (16).

Of particular interest are the phases θ_α. Owing to the second term on the rhs. of Eq. (27), these phases are

coupled to the phases of $\delta_{\mathbf{Q}\alpha}$. Let us analyze the possible values of the phases of the static lattice distortion. We first note that every $\mathbf{Q}_\alpha$ is half a reciprocal lattice vector in the normal phase, i.e., $e^{2i\mathbf{Q}_\alpha\mathbf{R}_i} = 1$, where $\mathbf{R}_i$ is a lattice vector of the undistorted lattice. Hence

$$b^\dagger_{\mathbf{Q}_\alpha} = \frac{1}{\sqrt{N}}\sum_i b_i^\dagger e^{-i\mathbf{Q}_\alpha\mathbf{R}_i} = \frac{1}{\sqrt{N}}\sum_i b_i^\dagger e^{-i\mathbf{Q}_\alpha\mathbf{R}_i+2i\mathbf{Q}_\alpha\mathbf{R}_i} = \frac{1}{\sqrt{N}}\sum_i b_i^\dagger e^{i\mathbf{Q}_\alpha\mathbf{R}_i} = b^\dagger_{-\mathbf{Q}_\alpha}\,. \tag{28}$$

That is $b^\dagger_{\mathbf{Q}\alpha}$ and $b^\dagger_{-\mathbf{Q}_\alpha}$ create the same phonon. This implies $\langle b^\dagger_{\mathbf{Q}_\alpha}\rangle = \langle b^\dagger_{-\mathbf{Q}_\alpha}\rangle = \langle b_{\mathbf{Q}_\alpha}\rangle$, and $\langle b_{\mathbf{Q}_\alpha}\rangle$ becomes a real number. The phase of $\delta_{\mathbf{Q}\alpha}$ is then exclusively determined by the corresponding phase of the electron-phonon coupling constant Φ_α, cf. Eqs. (25) and (26). However, since a triple CDW is not a simple superposition of three single CDWs the situation is more subtle. Here the change of the periodicity of the lattice caused by one CDW component affects the formation of the other two components. To elucidate this in some more detail let us assume that phonon 1 softens at T_c, while phonon 2 and phonon 3 soften at $T_c - \delta T$. As a result of the transition 1 at T_c the periodicity of the crystal changes and consequently the BZ changes too (cf. Fig. 4). The

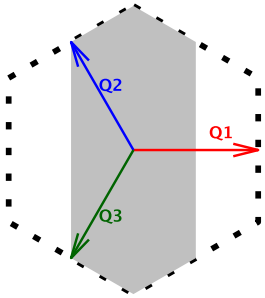

FIG. 4. (color online) BZ in the normal phase (black dotted hexagon) and (artificial) BZ that would emerge if only the phonon $\mathbf{Q}_1$ softens (filled gray hexagon). Red, green, and blue arrows indicate the ordering vectors $\mathbf{Q}_1$, $\mathbf{Q}_2$, and $\mathbf{Q}_3$, respectively.

vectors $\mathbf{Q}_2$ and $\mathbf{Q}_3$ are no longer half-reciprocal lattice vectors and Eq. (28) does not apply. Hence, at $T_c - \delta T$, $\langle b_{\mathbf{Q}2}\rangle$ and $\langle b_{\mathbf{Q}3}\rangle$ are complex numbers with phases that have to be determined by minimizing the free energy. For $1T$-$TiSe_2$, $\delta T = 0$, but nevertheless the above discussion remains valid. That is the freedom to fix the phases of the lattice distortions in an appropriate way results from the fact that one triple-CDW component must develop in a lattice structure which is already distorted by the other two triple-CDW components.

Based on the model (27), at zero temperature, we can relate the phases of $\delta_{\mathbf{Q}\alpha}$ and $\sum_{\mathbf{k}}\langle c^\dagger_{\mathbf{k}+\mathbf{Q}_\alpha\alpha}f_{\mathbf{k}}\rangle$. The ground-state energy per site is

$$\begin{aligned}\frac{\bar{E}}{N} = {}& \frac{2}{N}\sum_{\mathbf{k},\alpha}|\delta_{\mathbf{Q}\alpha}||\langle c^\dagger_{\mathbf{k}+\mathbf{Q}_\alpha\alpha}f_{\mathbf{k}}\rangle|\cos(\theta_\alpha-\phi_\alpha)\\ &+\frac{4D}{g^4_{\mathbf{Q}}}\sum_\alpha\sum_{\beta>\alpha}|\delta_{\mathbf{Q}\alpha}|^2|\delta_{\mathbf{Q}\beta}|^2\cos(2\phi_\alpha-2\Phi_\alpha)\\ &\times\cos(2\phi_\beta-2\Phi_\beta)+\frac{\widetilde{D}}{g^4_{\mathbf{Q}}}\sum_\alpha|\delta_{\mathbf{Q}\alpha}|^4\\ &+\sum_\alpha\hbar\omega\frac{|\delta_{\mathbf{Q}\alpha}|^2}{4(g_{\mathbf{Q}})^2}+\frac{\bar{E}_{\mathrm{mEFKM}}}{N}\,.\end{aligned} \tag{29}$$

The first term on the rhs. of Eq. (29) is minimized with

$$\theta_\alpha - \phi_\alpha = \pi \;\; + s\cdot 2\pi, \quad s = 0,1,2,... \tag{30}$$

We find that the phases θ_α are locked to $\phi_\alpha + (2s+1)\pi$. Thus, the phase relationship between ϕ_1, ϕ_2, and ϕ_3 is crucial. According to Eq. (29) only the term coming from the explicit phonon-phonon interaction, i.e., the second term on the rhs., will affect these phases. Neglecting the phonon-phonon interaction ϕ_1, ϕ_2, and ϕ_3 are independent of each other and chiral and standard CDWs are degenerate. So the particular form of $H_{\mathrm{ph-ph}}$ is essential in order to obtain a chiral CDW.

C. Self-consistency equations

Proceeding further, we assume that the electron-phonon interaction constants are real, i.e., $\Phi_1 = \Phi_2 = \Phi_3 = 0$. Taking into account the symmetry of the conduction bands and the equality of the electron-phonon interactions, we have $|\delta_{\mathbf{Q}1}| = |\delta_{\mathbf{Q}2}| = |\delta_{\mathbf{Q}3}| = |\delta_{\mathbf{Q}}|$ and $|\Delta_{\mathbf{Q}1}| = |\Delta_{\mathbf{Q}2}| = |\Delta_{\mathbf{Q}3}| = |\Delta_{\mathbf{Q}}|$. Therewith the free energy follows as

$$\begin{aligned}F = {}& \frac{1}{\beta N}\sum_{\mathbf{k},\nu}\ln(1-n_{\mathbf{k}\nu})+\mu+\frac{3\hbar\omega}{4(g_{\mathbf{Q}})^2}|\delta_{\mathbf{Q}}|^2\\ &-U_{fc}n_f\sum_\alpha n_\alpha - U_{cc}\sum_\alpha\sum_{\beta>\alpha}n_\alpha n_\beta+\frac{3}{U_{fc}}|\Delta_{\mathbf{Q}}|^2\\ &+\frac{4D}{g^4_{\mathbf{Q}}}|\delta_{\mathbf{Q}}|^4\Big[\cos(2\phi_1)\cos(2\phi_2)+\cos(2\phi_1)\cos(2\phi_3)\\ &+\cos(2\phi_2)\cos(2\phi_3)\Big]+\frac{3\widetilde{D}}{g^4_{\mathbf{Q}}}|\delta_{\mathbf{Q}}|^4,\end{aligned} \tag{31}$$

where $n_{\mathbf{k}\nu} = \left[1+e^{\beta(E_{\mathbf{k}\nu}-\mu)}\right]^{-1}$. The quasiparticle energies $E_{\mathbf{k}\nu}$ are obtained by diagonalizing the Hamilton matrix

$$[H] = \begin{pmatrix}\bar{\varepsilon}_{\mathbf{k}f} & \tilde{\Delta}^*_{\mathbf{Q}1} & \tilde{\Delta}^*_{\mathbf{Q}2} & \tilde{\Delta}^*_{\mathbf{Q}3}\\ \tilde{\Delta}_{\mathbf{Q}1} & \bar{\varepsilon}_{\mathbf{k}+\mathbf{Q}_1 1} & 0 & 0\\ \tilde{\Delta}_{\mathbf{Q}2} & 0 & \bar{\varepsilon}_{\mathbf{k}+\mathbf{Q}_2 2} & 0\\ \tilde{\Delta}_{\mathbf{Q}3} & 0 & 0 & \bar{\varepsilon}_{\mathbf{k}+\mathbf{Q}_3 3}\end{pmatrix}. \tag{32}$$

Evidently the three conduction bands are coupled to each other via their coupling to the single valence band. The resulting quasiparticle band structure exhibits a gap, whose magnitude is determined by the squared modulus of the "gap parameter"

$$\tilde{\Delta}_{\mathbf{Q}\alpha} = \delta_{\mathbf{Q}\alpha} - \Delta_{\mathbf{Q}\alpha}. \tag{33}$$

Naturally the relation (30) maximizes the gap parameter $|\tilde{\Delta}_{\mathbf{Q}\alpha}|$ for every given $|\delta_{\mathbf{Q}\alpha}|$ and $|\Delta_{\mathbf{Q}\alpha}|$. On the other hand, $E_{\mathbf{k}\nu}$ depends, via $\cos(\theta_\alpha - \phi_\alpha)$, on the phase differences only, i.e., the quasiparticle band structure can not be used to fix the particular values of θ_1, θ_2, and θ_3. We further note that $|\Delta_{\mathbf{Q}}| > 0$ if and only if $|\delta_{\mathbf{Q}}| > 0$. To elaborate let us first consider the case $g_{\mathbf{Q}} = 0$. In the EI phase ($|\Delta_{\mathbf{Q}}| > 0$) the system realizes a CDW. When $g_{\mathbf{Q}}$ becomes finite in addition, the lattice adjusts commensurate with the electron density modulation. Hence, in this case, any finite $g_{\mathbf{Q}}$ immediately results in $|\delta_{\mathbf{Q}}| > 0$. On the contrary, at vanishing Coulomb interaction but sufficiently large $g_{\mathbf{Q}} > g_{\mathbf{Q},c}$, a lattice instability develops leading to a finite $\sum_{\mathbf{k}}\langle c^\dagger_{\mathbf{k}+\mathbf{Q}_\alpha\alpha} f_{\mathbf{k}}\rangle$. This hybridization parameter enters the explicit equation for the EI order parameter (12). $|\Delta_{\mathbf{Q}}| > 0$ then follows from any finite Coulomb interaction. Our approach therefore does not discriminate between an excitonic and phonon-driven instability if both electron-electron and electron-phonon interactions are at play.

We now relate $|\Delta_{\mathbf{Q}}|$ and $|\delta_{\mathbf{Q}}|$. Minimizing F, Eq. (31), with respect to θ_α yields the constraint (30). This entails that the gap parameter is given by $|\tilde{\Delta}_{\mathbf{Q}\alpha}| = |\delta_{\mathbf{Q}}| + |\Delta_{\mathbf{Q}}|$. Depending on the sign of D, a different phase relationship between ϕ_1, ϕ_2, and ϕ_3 will be favored. For $D > 0$ we find that one phase has to be a multiple of π and another phase must be an odd multiple of $\pi/2$. The third phase is arbitrary. In this case the considered phonon-phonon interaction introduces a fixed phase difference between the lattice distortion modes. That is, $\theta_1 \neq \theta_2 \neq \theta_3$, and we observe a chiral CDW. On the other hand, for $D < 0$, F takes its minimum if all phases are a multiple $\pi/2$. The resulting CDW is then nonchiral. For both cases ($D > 0$ and $D < 0$), the free energy is minimized at finite values of $|\delta_{\mathbf{Q}}|$ if the constraint

$$\widetilde{D} \geq 4|D| \tag{34}$$

is fulfilled. Since the experiments suggest a chiral CDW, we take $D > 0$. Without loss of generality we further set $\phi_1 = 0$, $\phi_2 = \pi/2$, $\phi_3 = 3\pi/10$, and assume $\widetilde{D} = 4D$. The modulii of $|\delta_{\mathbf{Q}}|$ and $|\Delta_{\mathbf{Q}}|$ are then determined by $\partial F/\partial|\delta_{\mathbf{Q}}| = 0$ and $\partial F/\partial|\Delta_{\mathbf{Q}}| = 0$, respectively. Straightforward calculation gives

$$\begin{aligned}\frac{3}{U_{fc}}|\Delta_{\mathbf{Q}}| = \frac{3\hbar\omega}{4g^2_{\mathbf{Q}}}|\delta_{\mathbf{Q}}| + 8\frac{D}{g^4_{\mathbf{Q}}}|\delta_{\mathbf{Q}}|^3\Big[&\cos(2\phi_1)\cos(2\phi_2) \\ &+ \cos(2\phi_1)\cos(2\phi_3) + \cos(2\phi_2)\cos(2\phi_3)\Big] \\ &+ 6\frac{\widetilde{D}}{g^4_{\mathbf{Q}}}|\delta_{\mathbf{Q}}|^3.\end{aligned} \tag{35}$$

Let us finally stress that we can only specify values for the phases θ_α and ϕ_α. Which particular phase takes one of these values remains open. For instance, the simultaneous transformations $\theta_2 \to \theta_3$ and $\phi_2 \to \phi_3$ do not change the free energy, but convert a clockwise chiral CDW in an anticlockwise one. The degeneracy of these two CDW states is in accord with the experimental findings for $1T$-$TiSe_2$.[5]

D. Characterization of the CDW state in $1T$-$TiSe_2$

Experiments identify a close connection between the appearance of the CDW state and the periodic lattice displacement in $1T$-$TiSe_2$.[7] In the scheme developed in the preceding sections the CDW is directly accompanied by a lattice distortion. There the j-component ($j = x, y, z$) of the lattice deformation caused by the phonon α is

$$\tilde{u}^\alpha_j(\mathbf{r}) = \frac{1}{\sqrt{N}}\sum_l \sqrt{\frac{2\hbar}{\omega M_l}}|\langle b^\dagger_{\mathbf{Q}_\alpha}\rangle|\,\epsilon_{l,j}(\mathbf{Q}_\alpha)\,\cos(\mathbf{Q}_\alpha\mathbf{r} - \phi_{b\alpha}), \tag{36}$$

where $\epsilon_{l,j}(\mathbf{Q}_\alpha)$ is the j-component of the polarization vector, l labels the atoms in the unit cell, and M_l is the mass of the atom l. Clearly each CDW component α produces a 3D lattice distortion. Since $\phi_{b1} \neq \phi_{b2} \neq \phi_{b3}$ if $\phi_1 \neq \phi_2 \neq \phi_3$, the lattice will be differently affected by the phonons $\mathbf{Q}_1$, $\mathbf{Q}_2$, and $\mathbf{Q}_3$. Of course the lattice deformation by the phonon mode $\mathbf{Q}_\alpha$ is position-dependent; in this way a complicated distortion pattern of the ions can occur. An instructive picture can be achieved, however, if one neglects the $\mathbf{r}$-dependence in the xy-plane. In this simplified situation, depending on the z-component as a function of $\mathbf{r}$, the magnitude of the lattice displacement differs along $\mathbf{Q}_1$, $\mathbf{Q}_2$, and $\mathbf{Q}_3$. As a result the different ionic layers of $1T$-$TiSe_2$ are dominated by different phonon modes.[7] The situation where the lower Se-ion layer is largely affected by the phonon mode $\mathbf{Q}_3$, the Ti-ion layer by phonons with momentum $\mathbf{Q}_2$, and the upper Se-ion layer by the $\mathbf{Q}_1$ phonon mode, is illustrated schematically in Fig. 5(a). Let us consider the upper

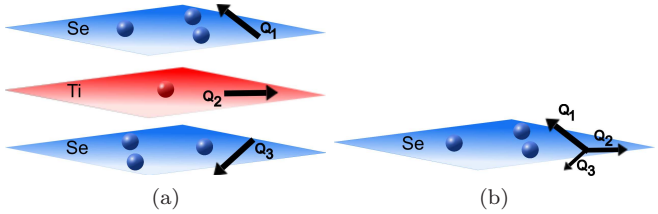

FIG. 5. (color online) (a) For a chiral ordering the maximum lattice distortion due to the phonon $\mathbf{Q}_\alpha$ may be located in different ionic layers. (b) The Se ions in the upper layer are differently affected by the phonons having momentum $\mathbf{Q}_1$, $\mathbf{Q}_2$, or $\mathbf{Q}_3$. For further discussion see text.

plane of Se ions, which is analyzed in scanning tunneling microscopy experiments.[5] There a relative difference of

the phases $\phi_{b\alpha}$ leads, e.g., to a stronger displacement of the ions in the direction of $\mathbf{Q}_1$ than in the direction of $\mathbf{Q}_2$ and $\mathbf{Q}_3$ [see Fig. 5(b)]. Then the CDW transition can be viewed as a formation of "virtual layers" with ordering vectors assigned to a helical structure.[5] The described distortion scenario equates with a fixed phase difference. Thereby the only crucial parameters are ϕ_1, ϕ_2, and ϕ_3; the finite z-component of the ordering vectors is not a required prerequisite for the chiral CDW.

We add that in our model both CDW transitions appear simultaneously, i.e., $T_{\mathrm{CDW}} = T_{\mathrm{chiral}}$. This contradicts the result $T_{\mathrm{chiral}} < T_{\mathrm{CDW}}$ by van Wezel.[7,8] In that Landau-Ginzburg approach terms of second and quartic order in the order parameter appear. While the second-order term favors equal phases, the quartic-order term supports a phase difference.[7] Hence there is a competition between a nonchiral and a chiral CDW state. This competition is absent in our approach where we have only a single term that fixes the values of ϕ_1, ϕ_2, ϕ_3 respectively θ_1, θ_2, θ_3. Very recent X-ray diffraction and electrical transport measurements provide some evidence that the transition to the chiral CDW takes place at lower temperature than the CDW transition.[50] The difference between T_{CDW} and T_{chiral} is less than ten Kelvin however. Having disregarded fluctuation corrections, which are known to play an important role in the vicinity of a phase transition, we can not conclusively resolve this issue.

III. NUMERICAL RESULTS

A. Model assumptions

In view of the quasi-2D crystallographic and electronic structure of $1T$-$TiSe_2$, and in order to simplify the numerics, we restrict the following analysis to a strictly 2D setting. Moreover, being close to the Fermi energy, we will approximate the bands parabolically[10]

$$\varepsilon_{\mathbf{k}f} = -t_f \left(k_x^2 + k_y^2\right), \tag{37}$$

$$\varepsilon_{\mathbf{k}1} = t_c^x (k_x - Q_{1x})^2 + t_c^y (k_y - Q_{1y})^2 + E_c, \tag{38}$$

with hopping amplitudes t_f, t_c^x, and t_c^y. The other two conduction bands $\varepsilon_{\mathbf{k}2}$ and $\varepsilon_{\mathbf{k}3}$ have analogous dispersions, but the momenta are rotated by $2\pi/3$ and $4\pi/3$, respectively. All three conduction bands share the same minimum E_c, see Fig. 3.

From the band dispersion provided by Monney *et al.* in Ref. 10 we derive $t_f = 1.3$ eV, which will be taken as the unit of energy hereafter, and $t_c^x = 0.042$ and $t_c^y = 0.105$. The bare phonon frequency is estimated as $\hbar\omega = 0.013$, in accordance with the value given by Weber *et al.* in Ref. 20. Furthermore, we set $E_c = -3.30$ and $U_{cc} = U_{fc} + 1.0$. For the phonon-phonon interaction constant we take $D = 10^{-4}$.

The self-consistency loop, comprising the determination of the EI order parameter, the static lattice distortion, the total and partial particle densities and the chemical potential, is solved iteratively until the relative error of each physical quantity is less than 10^{-6}. The numerical integrations were performed using the Cubpack package.[51]

B. Phase diagram of the mEFKM

To set the stage for the analysis of the interplay of Coulomb and electron-phonon interaction effects we first discuss the phase diagram of the pure mEFKM, cf. Fig. 6. Here, since $g_{\mathbf{Q}} = 0$ (and as a result $\delta_{\mathbf{Q}\alpha} = 0$), the EI low-temperature phase typifies a normal CDW. As for the EFKM on a square lattice (see inset), at $T = 0$ we find a finite critical Coulomb strength above which the EI phase does not exist. This is because the large band splitting caused by the Hartree term of the Coulomb interaction prevents c-f electron coherence.[42] In contrast

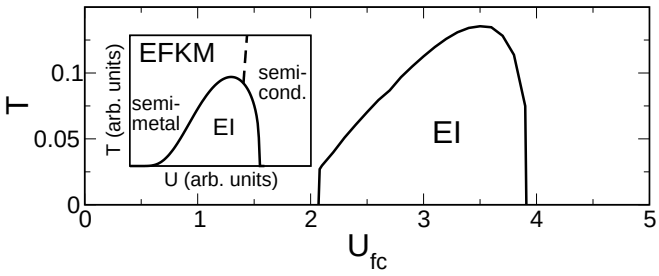

FIG. 6. Phase diagram of the mEFKM. The inset displays the schematic phase diagram of the simplified two-band EFKM on a square lattice according to Ref. 42.

to the EFKM, in our four-band model we also find a critical lower Coulomb strength for the EI phase. This can be understood as follows: since the valence band is isotropic while the conduction-band dispersions are strongly anisotropic, particles close to the Fermi level do not find a large number of partners with appropriate momentum for electron-hole pairing. Thus, for U_{fc} smaller than a critical Coulomb attraction, the amount of energy to create a macroscopic number of excitons is larger than the energy gain from the condensation transition into the EI state. Therefore the system remains in the semimetallic phase.[52] The rather abrupt increase of the critical temperature at the lower critical Coulomb interaction is due to the degeneracy of of the conduction bands and the particular anisotropy used.

C. Influence of the lattice degrees of freedom

We now analyze the situation when phonons participate in the CDW formation. In Fig. 7 we consider the dependence of the EI order parameter $|\Delta_{\mathbf{Q}}|$ and the static lattice distortion $|\delta_{\mathbf{Q}}|$ on the interaction constants at $T = 0$. For small electron-phonon coupling the behavior of the EI order parameter resembles the situation for the mEFKM (EI limit). Differences appear for

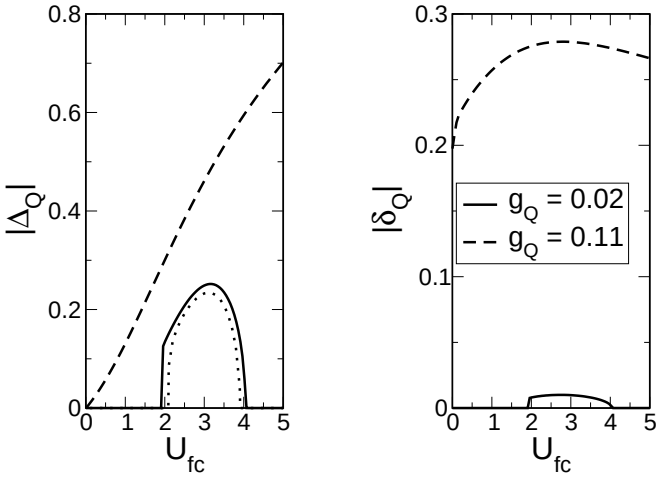

FIG. 7. EI order parameter $|\Delta_{\mathbf{Q}}|$ (left panel) and static lattice distortion $|\delta_{\mathbf{Q}}|$ (right panel) as a function of the Coulomb interaction U_{fc} at $T = 0$. Results are given for $g_{\mathbf{Q}} = 0.02$ (solid lines) and $g_{\mathbf{Q}} = 0.11$ (dashed lines). For comparison, in the left-hand panel, the EI order parameter of the pure mEFKM is included ($g_{\mathbf{Q}} = 0$; dotted line).

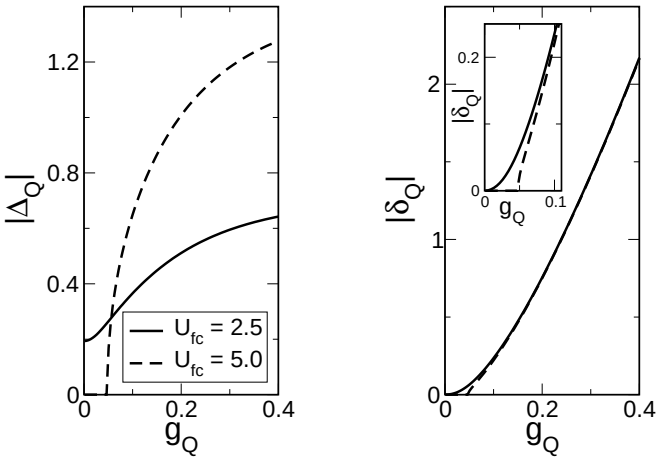

FIG. 8. EI order parameter $|\Delta_{\mathbf{Q}}|$ (left panel) and static lattice distortion $|\delta_{\mathbf{Q}}|$ (right panel) as a function of the electron-phonon coupling $g_{\mathbf{Q}}$ at $T = 0$. Results are given for $U_{fc} = 2.5$ (solid lines) and $U_{fc} = 5.0$ (dashed lines). The right-hand inset enlarges the region of small $g_{\mathbf{Q}}$.

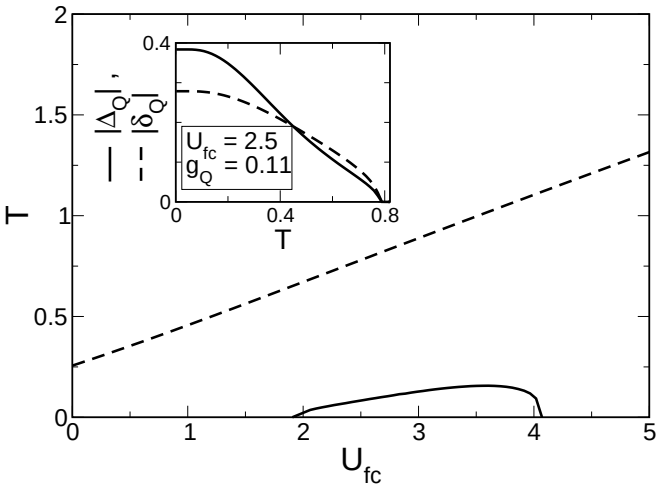

FIG. 9. CDW phase boundaries for $g_{\mathbf{Q}} = 0.02$ (solid line) and $g_{\mathbf{Q}} = 0.11$ (dashed line). The inset gives the EI order parameter (solid line) and the static lattice distortion (dashed line) as a function of temperature for $g_{\mathbf{Q}} = 0.11$ at $U_{fc} = 2.5$.

$g_{\mathbf{Q}} = 0.11$ where we do not find a lower critical U_{fc} for the CDW phase, i.e., now any finite U_{fc} leads to a finite $|\Delta_{\mathbf{Q}}|$. The order parameter $|\Delta_{\mathbf{Q}}|$ shows an almost linear dependence on U_{fc}, which means that the electron-hole pairing probability ($\propto |\Delta_{\mathbf{Q}}|/U_{fc}$) remains approximately constant. The tendency towards exciton formation and condensation is notably enhanced as $g_{\mathbf{Q}}$ increases at fixed U_{fc}. The static lattice distortion is tiny and follows the behavior of the EI order parameter for small $g_{\mathbf{Q}}$. For $g_{\mathbf{Q}} = 0.11$ we observe a non-monotonic behavior of $|\delta_{\mathbf{Q}}|$ as a function of the electron-electron interaction. At very large electron-phonon couplings the influence of the electron-electron interaction on $|\delta_{\mathbf{Q}}|$ weakens (not shown in Fig. 7).

Figure 8 gives the dependence of the order parameters on the electron-phonon coupling constant at fixed U_{fc}. For $U_{fc} = 2.5$ the order parameters remain finite as $g_Q \to 0$ since we already have a CDW in the pure mEFKM (see Fig. 6). A Coulomb strength $U_{fc} = 5.0$, on the other hand, does not lead to an EI if phonons are absent. Then we find a lower critical $g_{\mathbf{Q}}$. Furthermore we observe a saturation of the EI order parameter with increasing $g_{\mathbf{Q}}$, since $|\Delta_{\mathbf{Q}}|$ is limited by the number of electrons that can participate in the electron-hole pairing. Within our approximation the expectation value of the phonon-creation operator is not bounded and $|\delta_{\mathbf{Q}}|$ continuously increases with enhanced electron-phonon coupling. Note that an increasing phonon-phonon interaction strength D reduces the static lattice distortion and therefore leads to a smaller EI order parameter (not shown).

Finite temperature effects are illustrated in Fig. 9. For very small electron-phonon coupling the phase diagram again resembles the situation for the mEFKM. As the interaction strength $g_{\mathbf{Q}}$ increases the situation changes dramatically. For sufficiently large electron-phonon couplings, we no longer find critical lower and upper values U_{fc} for the CDW transition and the transition temperature increases linearly with U_{fc}. That is the critical temperature is significantly enhanced by $g_{\mathbf{Q}}$. Obviously electron-hole attraction and electron-phonon coupling act together in the formation of a very stable CDW phase. The inset shows how the order parameters are suppressed by increasing temperature. Here the static lattice distortion reveals a typical mean-field dependence.

Our findings are summarized by the ground-state phase diagram shown in Fig. 10. For weak electron-phonon couplings $g_{\mathbf{Q}}$ the CDW is mainly driven by the

Coulomb attraction U_{fc} between electrons and holes. The greater $g_{\mathbf{Q}}$, the larger the region where the CDW is stable. For $g_{\mathbf{Q}} > 0.09$ the electron-phonon coupling alone can cause the CDW transition, even at $U_{fc} = 0$ (blue line in Fig. 10). The CDW is chiral in this limit, whereas the CDW in the opposite EI limit does not exhibit chirality ($g_{\mathbf{Q}} = 0$, red line in Fig. 10).

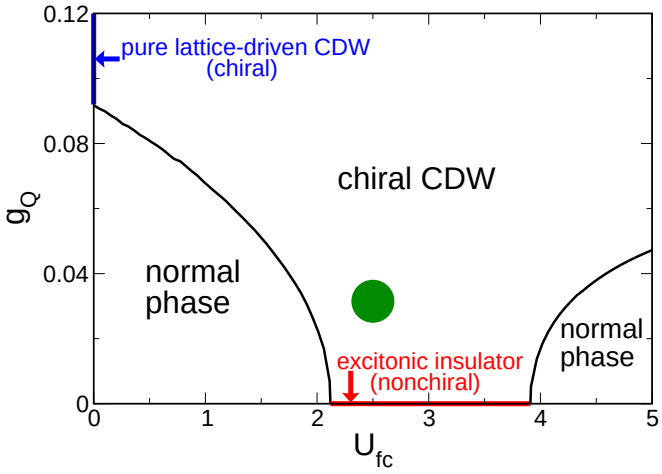

FIG. 10. (color online) Ground-state phase diagram of the mEFKM with additional electron-phonon coupling. The CDW phase is characterized by a finite gap parameter $|\tilde{\Delta}_{\mathbf{Q}}|$. The red line at $g_{\mathbf{Q}} = 0$ marks the EI phase of the pure mEFKM. The blue line at $U_{fc} = 0$ refers to a CDW induced solely by the electron-lattice interaction. The green point designates the range of model parameters appropriate for $1T$-$TiSe_2$.

D. Relation to $1T$-$TiSe_2$

Based on the phase diagram derived for the mEFKM with electron-phonon coupling, we now attempt to estimate the electron-electron and electron-phonon interaction constants, U_{fc} and $g_{\mathbf{Q}}$, for $1T$-$TiSe_2$. To make contact with the experiments we take the displacements of the Ti ions measured by Di Salvo *et al.*: $\tilde{u}_{l=\mathrm{Ti}} = 0.04\mathring{A}$ with $\tilde{u} = \sum_l \tilde{u}_l$.[4] Then, from Eq. (36), we can specify the value of $|\langle b^\dagger_{\mathbf{Q}} \rangle|$. For $1T$-$TiSe_2$, the gap parameter was determined experimentally as 120 meV by Monney *et al.*, cf. Ref. 44. Adjusting this value to our theoretical results yields $U_{fc} \approx 2.5$ (≈ 3 eV) and $g_{\mathbf{Q}} \approx 0.03$ (≈ 0.04 eV); see the green marker in Fig. 10. For these values both the theoretical ion displacement and gap parameter are in the same order of magnitude as the measured ones. Using $U_{fc} \approx 2.5$ for $1T$-$TiSe_2$, the electron-hole pairing is BCS-like. Since $g_{\mathbf{Q}} \simeq 0.03$ is too small to cause a CDW for vanishing Coulomb interaction and, as discussed above, the EI scenario alone will not yield a stable chiral CDW, our results are in favor of a combined lattice-deformation/EI mechanism for the experimentally observed chiral CDW transition, as suggested in Refs. 22 and 53.

IV. CONCLUSIONS

In this work we have argued how the chiral charge-density-wave (CDW) phase in $1T$-$TiSe_2$ may be stabilized. In the framework of the multiband extended Falicov-Kimball model (mEFKM) we showed that a purely electronic—exciton pairing and condensation—mechanism is insufficient to induce the observed (long-ranged) chiral charge order. We propose that the coupling of the electrons to the lattice degrees of freedom is essential for the formation of a chiral CDW state. In particular, an explicit phonon-phonon interaction between the phonons that become soft at the critical temperature has to be taken into account in order to stabilize the chiral CDW. We note that in our model clockwise and anticlockwise CDWs are degenerate. This is in accord with experimental findings.[5] The chiral property can properly be observed in the ionic displacements accompanying the CDW in $1T$-$TiSe_2$.

Concerning the microscopic mechanism underlying the CDW transition, we demonstrated that electron-electron interaction and electron-phonon coupling support each other in driving the electron-hole pairing and finally the instability. This suggests that the CDW transition in $1T$-$TiSe_2$ is due to a combined lattice distortion and exciton-condensation effect. The outcome is a spontaneous broken-symmetry CDW low-temperature state with small but finite lattice deformation. Of course, both the mean-field treatment of the Coulomb interaction and the frozen-phonon approach are rather crude approximations and a more elaborated study of the complex interplay between the electronic and phononic degrees of freedom is highly desirable to confirm our proposed scenario for the chiral CDW transition in $1T$-$TiSe_2$.

Let us finally point out that we called $|\Delta_{\mathbf{Q}}|$ the excitonic-insulator order parameter on account of its analog in the EFKM.[35–42] The meaning of a finite $|\Delta_{\mathbf{Q}}|$ in the presence of a band coupling is imprecise however. Likewise a spontaneous hybridization of the valence band with one of the conduction bands, signaling the exciton condensate in the mEFKM, may be induced by a sufficiently large electron-phonon coupling. A general criterion for the formation of an exciton condensate in a strongly coupled band situation has not been established so far. This is an open issue which deserves further analysis because of its relevance in characterizing the nature of CDW transitions also in other materials.[54,55]

ACKNOWLEDGMENTS

We thank P. Aebi, K. W. Becker, F. X. Bronold, D. Ihle, G. Monney, and P. V. Nham for valuable discussions. This work is supported by the Deutsche Forschungsgemeinschaft through SFB 652 (project B5),

by the Fonds National Suisse pour la Recherche Scientifique through Div. II, the Swiss National Center of Competence in Research MaNEP, and the U.S. Department of Energy. C.M. acknowledges also support by the Fonds National Suisse pour la Recherche Scientifique under grant PA00P2-142054.

[1] R. Peierls, *Quantum theory of solids* (Oxford University Press, Oxford, 1955).
[2] J. Sólyom, Adv. Phys. **28**, 201 (1979).
[3] G. Grüner, *Density Waves in Solids* (Perseus Publishing, 2000).
[4] F. J. Di Salvo, D. E. Moncton, and J. V. Waszczak, Phys. Rev. B **14**, 4321 (1976).
[5] J. Ishioka, Y. H. Liu, K. Shimatake, T. Kurosawa, K. Ichimura, Y. Toda, M. Oda, and S. Tanda, Phys. Rev. Lett. **105**, 176401 (2010).
[6] J. van Wezel and P. Littlewood, Physics **3**, 87 (2010).
[7] J. van Wezel, Europhys. Lett. **96**, 67011 (2011).
[8] J. van Wezel, Physica B **407**, 1779 (2012).
[9] H. Cercellier, C. Monney, F. Clerc, C. Battaglia, L. Despont, M. G. Garnier, H. Beck, P. A. ans L. Patthey, H. Berger, and L. Forró, Phys. Rev. Lett. **99**, 146403 (2007).
[10] C. Monney, H. Cercellier, F. Clerc, C. Battaglia, E. F. Schwier, C. Didiot, M. G. Garnier, H. Beck, P. Aebi, H. Berger, L. Forró, and L. Patthey, Phys. Rev. B **79**, 045116 (2009).
[11] C. Monney, C. Battaglia, H. Cercellier, P. Aebi, and H. Beck, Phys. Rev. Lett. **106**, 106404 (2011).
[12] M. M. May, C. Brabetz, C. Janowitz, and R. Manzke, Phys. Rev. Lett. **107**, 176405 (2011).
[13] T. Rohwer, S. Hellmann, M. Wiesenmayer, C. Sohrt, A. Stange, B. Slomski, A. Carr, Y. Liu, L. M. Avila, M. Kalläne, S. Mathias, L. Kipp, K. Rossnagel, and M. Bauer, Nature **471**, 490 (2011).
[14] H. P. Hughes, J. Phys. C **10**, L319 (1977).
[15] K. Rossnagel, L. Kipp, and M. Skibowski, Phys. Rev. B **65**, 235101 (2002).
[16] Y. Yoshida and K. Motizuki, J. Phys. Soc. Japan **49**, 898 (1980).
[17] K. Motizuki, N. Suzuki, Y. Yoshida, and Y. Takaoka, Solid State Commun. **40**, 995 (1981).
[18] N. Suzuki, A. Yamamoto, and K. Motizuki, J. Phys. Soc. Japan **54**, 4668 (1985).
[19] M. Holt, P. Zschack, H. Hong, M. Y. Chou, and T. C. Chiang, Phys. Rev. Lett. **86**, 3799 (2001).
[20] F. Weber, S. Rosenkranz, J.-P. Castellan, R. Osborn, G. Karapetrov, R. Hott, R. Heid, K.-P. Bohnen, and A. Alatas, Phys. Rev. Lett. **107**, 266401 (2011).
[21] M. Calandra and F. Mauri, Phys. Rev. Lett. **106**, 196406 (2011).
[22] J. van Wezel, P. Nahai-Williamson, and S. S. Saxena, Europhys. Lett. **89**, 47004 (2010).
[23] C. Monney, G. Monney, P. Aebi, and H. Beck, New J. Phys. **14**, 075026 (2012).
[24] J. Neuenschwander and P. Wachter, Phys. Rev. B **41**, 12693 (1990).
[25] P. Wachter and B. Bucher, Physica B **408**, 51 (2013).
[26] K. Kanda, K. Machida, and T. Matsubara, Solid State Commun. **19**, 651 (1976).
[27] T. Portengen, T. Östreich, and L. J. Sham, Phys. Rev. Lett. **76**, 3384 (1996).
[28] C. D. Batista, Phys. Rev. Lett. **89**, 166403 (2002).
[29] N. F. Mott, Philos. Mag. **6**, 287 (1961).
[30] R. Knox, in *Solid State Physics*, edited by F. Seitz and D. Turnbull (Academic Press, New York, 1963) p. Suppl. 5 p. 100.
[31] D. Jérome, T. M. Rice, and W. Kohn, Physical Review **158**, 462 (1967).
[32] F. X. Bronold and H. Fehske, Phys. Rev. B **74**, 165107 (2006).
[33] C. D. Batista, J. E. Gubernatis, J. Bonča, and H. Q. Lin, Phys. Rev. Lett. **92**, 187601 (2004).
[34] P. Farkašovský, Phys. Rev. B **77**, 155130 (2008).
[35] C. Schneider and G. Czycholl, Eur. Phys. J. B **64**, 43 (2008).
[36] D. Ihle, M. Pfafferott, E. Burovski, F. X. Bronold, and H. Fehske, Phys. Rev. B **78**, 193103 (2008).
[37] B. Zenker, D. Ihle, F. X. Bronold, and H. Fehske, Phys. Rev. B **81**, 115122 (2010).
[38] V.-N. Phan, K. W. Becker, and H. Fehske, Phys. Rev. B **81**, 205117 (2010).
[39] B. Zenker, D. Ihle, F. X. Bronold, and H. Fehske, Phys. Rev. B **83**, 235123 (2011).
[40] V.-N. Phan, H. Fehske, and K. W. Becker, Europhys. Lett. **95**, 17006 (2011).
[41] K. Seki, R. Eder, and Y. Ohta, Phys. Rev. B **84**, 245106 (2011).
[42] B. Zenker, D. Ihle, F. X. Bronold, and H. Fehske, Phys. Rev. B **85**, 121102R (2012).
[43] C. Monney, E. F. Schwier, M. G. Garnier, N. Mariotti, C. Didiot, H. Cercellier, J. Marcus, H. Berger, A. N. Titov, H. Beck, and P. Aebi, New J. Phys. **12**, 125019 (2010).
[44] C. Monney, E. F. Schwier, M. G. Garnier, N. Mariotti, C. Didiot, H. Beck, P.Aebi, C. Cercellier, J. Marcus, C. Battaglia, H. Berger, and A. N. Titov, Phys. Rev. B **81**, 155104 (2010).
[45] M. Cazzaniga, H. Cercellier, M. Holzmann, C. Monney, P. Aebi, G. Onida, and V. Olevano, Phys. Rev. B **85**, 195111 (2012).
[46] C. Monney, G. Monney, P. Aebi, and H. Beck, Phys. Rev. B **85**, 235150 (2012).
[47] H. Ehrenreich and A. W. Overhauser, Phys. Rev. **104**, 331 (1956).
[48] J. M. Ziman, *Electrons and Phonons* (Clarendon, London, 1960).
[49] N. W. Ashcroft and N. D. Mermin, *Solid state physics* (Saunders College Publ. Philadelphia, 1976).
[50] J.-P. Castellan, S. Rosenkranz, R. Osborn, Q. Li, K. Gray, G. Karapetrov, J. Ruff, and J. van Wezel, (2012), preprint.
[51] R. Cools and A. Haegemans, ACM Transactions on Mathematical Software **29**, 287 (2003).
[52] J. Zittartz, Phys. Rev. **162**, 752 (1967).
[53] Z. Zhu, Y. Cheng, and U. Schwingenschlögl, Phys. Rev. B **85**, 245133 (2012).
[54] T. Kaneko, T. Toriyama, T. Konishi, and Y. Ohta, (2012), preprint.

824 [55] D. K. Efimkin, Y. E. Lozovik, and A. A. Sokolik, (2012), 825 preprint.